RESEARCH ARTICLE
doi: 10.2306/scienceasia1513-1874.2013.39.410

ScienceAsia 39 (2013): **410–415**

Contact infection spread in an SEIR model: An analytical approach

Puntani Pongsumpun[a,*], **Rujira Kongnuy**[a], **Diana García López**[b], **I-Ming Tang**[c], **Marc A. Dubois**[b]

[a] Department of Mathematics, Faculty of Science, King Mongkut's Institute of Technology Ladkrabang, Bangkok 10520 Thailand

[b] SPEC-CEA Saclay/CNRS URA 2464, Orme des Merisiers, 91191 Gif-sur-Yvette Cedex, France

[c] Department of Physics, Faculty of Science, Mahidol University, Rama 6 Road, Bangkok 10400 Thailand

*Corresponding author, e-mail: kppuntan@kmitl.ac.th

Received 22 Sep 2012
Accepted 27 May 2013

ABSTRACT: The epidemic spread of an SEIR (susceptible-exposed-infectious-recovered) model is analysed via a contact infection process. We solve the system of nonlinear partial differential equations by using the method of separation of variables. Approximate analytical expressions for the propagating infection wave for various ranges of parameters are presented.

KEYWORDS: infection wave, epidemic spread, diffusion

INTRODUCTION

The modelling of epidemics has been the object of a vast number of studies over the past century[1]. The desire to understand their mechanism has led to the formulation of models which make possible the simulation of events for which laboratory experiments cannot be conducted easily. Such approaches include reaction-diffusion models[2,3] and may include nonlinear incidence rates in compartmented models[4–9], use travelling waves equations[10,11] and non-local delayed terms[12].

The process of an epidemic spread in a population of individuals with low mobility within the susceptible-infectious-recovered (SIR) scheme was studied by Postnikov and Sokolov. In a continuum limit, such a propagation mechanism is described by a nonlinear reaction-diffusion equation with a diffusion coefficient that is a function of the density of susceptibles. The travelling wave solution of the corresponding system of partial differential equations has been obtained and analysed[13]. The spread of a contact infection following the SIR scheme through an immobile population with the slab geometry has been considered[14]. The choice of compartments to be included in a model depends upon the characteristics of the particular disease being modelled and the purpose of the model. In the SEIR model, the population is partitioned into four compartments at any time t: susceptible individuals $S(t)$ (individuals at risk of getting infection), infected individuals who are not yet infectious $E(t)$, infected individuals who are infectious (capable of transmitting the infection) $I(t)$, and recovered individuals $R(t)$ (those who have recovered from the infection after being infectious for a defined period).

Some diseases, such as the viral diseases SARS and measles but also several vector-mediated diseases like the four strains of dengue, need to be modelled using an SEIR approach. In this paper, we extend the study of Ref. 14 to analyse the infection wave solutions of an SEIR model instead of an SIR model and we try to complete the analytical study. We show the distribution of the infection waves for the different ranges of parameters, and compare it to the SIR behaviour.

THE MODEL AND ITS SOLUTIONS

Infection wave in a comoving frame: separation of variables

S, E, I and R are the fractions of the population in each state, and are functions of the space variable x as well as of time, and so $S + E + I + R = 1$. Each individual is assumed to be slowly moving with a high returning rate. Hence the propagation of the disease is a contact process where an infectious individual happens to encounter a susceptible one. As has been discussed by Kendall[3], and as is done in Refs. 13, 14, we consider the spatially averaged concentration of infected at the point where we compute the transition from susceptible to exposed. Applying the scheme of

Naether, Postnikov and Sokolov [13, 14], we obtain

$$\Delta E(x,y) = \frac{c}{4}S(x,y)[I(x+b,y) + I(x-b,y) + I(x,y+b) + I(x,y-b)]\Delta t, \quad (1)$$

where c is the contact rate and b is the lattice spacing. After we expand terms in brackets in (1) by using a Taylor series expansion about (x,y) up to the first non-vanishing term in b, we get the partial differential equation

$$\frac{\partial E}{\partial t} = cSI + DS\frac{\partial^2 I}{\partial x^2} \quad (2)$$

where $D = cb^2/4$. It should be emphasized that D is not a diffusion coefficient of individuals but comes from the Taylor expansion of the average of contacts around the point considered.

The transition rate from exposed to infectious is proportional to E/τ, where τ is the intrinsic incubation time. Thus including this incubation term, one obtains

$$\frac{\partial E}{\partial t} = cSI - \frac{E}{\tau} + DS\frac{\partial^2 I}{\partial x^2}.$$

In the same way, the rate of infectious who recover is defined by I/s, where $(1/s)$ is the recovery rate of an infectious person. From the above assumptions, the basic mechanisms for the development and spatial spread of the disease are defined as follows:

$$\frac{\partial S}{\partial t} = -cSI - DS\frac{\partial^2 I}{\partial x^2} \quad (3)$$

$$\frac{\partial E}{\partial t} = cSI - \frac{E}{\tau} + DS\frac{\partial^2 I}{\partial x^2} \quad (4)$$

$$\frac{\partial I}{\partial t} = \frac{E}{\tau} - \frac{I}{s} \quad (5)$$

$$\frac{\partial R}{\partial t} = \frac{I}{s} \quad (6)$$

where $S + E + I + R = 1$.

As in Ref. 14, we consider a continuous description and the propagation of a stationary wave of infection. We change to a comoving frame $x' = x - vt$ where v is the velocity of the wave of infection.

$$-v\frac{\mathrm{d}S}{\mathrm{d}x'} = -cSI - DS\frac{\mathrm{d}^2 I}{\mathrm{d}x'^2} \quad (7)$$

$$-v\frac{\mathrm{d}E}{\mathrm{d}x'} = cSI - \frac{E}{\tau} + DS\frac{\mathrm{d}^2 I}{\mathrm{d}x'^2} \quad (8)$$

$$-v\frac{\mathrm{d}I}{\mathrm{d}x'} = \frac{E}{\tau} - \frac{I}{s} \quad (9)$$

$$-v\frac{\mathrm{d}R}{\mathrm{d}x'} = \frac{I}{s}. \quad (10)$$

Using the fact that $S + E + I + R = 1$ everywhere, one can rewrite (7) as

$$-v\frac{\mathrm{d}S}{\mathrm{d}x'} = -cS(1-S) + DS\frac{\mathrm{d}^2 S}{\mathrm{d}x'^2} + S\left(cR + D\frac{\mathrm{d}^2 R}{\mathrm{d}x'^2}\right) + S\left(cE + D\frac{\mathrm{d}^2 E}{\mathrm{d}x'^2}\right). \quad (11)$$

Returning to consider (7), after dividing both sides by $-S$, we obtain

$$v\frac{\mathrm{d}\ln S}{\mathrm{d}x'} = cI + D\frac{\mathrm{d}^2 I}{\mathrm{d}x'^2}. \quad (12)$$

If we substitute I in the right-hand side of (12), then

$$\frac{\mathrm{d}}{\mathrm{d}x'}\left[\ln S + s\left(cR + D\frac{\mathrm{d}^2 R}{\mathrm{d}x'^2}\right)\right] = 0.$$

This means that the initial system of equations possesses an integral of motion

$$\ln S + s\left(cR + D\frac{\mathrm{d}^2 R}{\mathrm{d}x'^2}\right) = c_0 \quad (13)$$

where c_0 is a constant.

Approximate solutions: leading front

To determine the value of the constant c_0, we consider $x \to \infty$, far in front of the infection wave. In this domain, $S = 1$ (and $\ln S = 0$), $R = 0 = \mathrm{d}^2R/\mathrm{d}x'^2$, $E = I = 0$, $\mathrm{d}^2E/\mathrm{d}x'^2 = \mathrm{d}^2I/\mathrm{d}x'^2 = 0$ so that $c_0 = 0$. Consequently,

$$\ln S + s\left(cR + D\frac{\mathrm{d}^2 R}{\mathrm{d}x'^2}\right) = 0. \quad (14)$$

After some calculations, we obtain the relation

$$E = v\tau\frac{\mathrm{d}S}{\mathrm{d}x'} + v^2\tau^2\frac{\mathrm{d}^2 S}{\mathrm{d}x'^2} + v^2\tau^2\frac{\mathrm{d}^2 E}{\mathrm{d}x'^2}. \quad (15)$$

Using the above relations, we can rewrite (11) as

$$-v\frac{\mathrm{d}S}{\mathrm{d}x'} = -cS(1-S) + DS\frac{\mathrm{d}^2 S}{\mathrm{d}x'^2} - \frac{1}{s}S\ln S + DS\frac{\mathrm{d}^2 E}{\mathrm{d}x'^2} + cv\tau S\frac{\mathrm{d}S}{\mathrm{d}x'} + v^2\tau^2 cS\frac{\mathrm{d}^2 S}{\mathrm{d}x'^2} + v^2\tau^2 cS\frac{\mathrm{d}^2 E}{\mathrm{d}x'^2}. \quad (16)$$

The second derivative in (16) at the front of the infection wave is small and can be neglected. Since S is still close to unity in front of the infection wave, one can use a Taylor expansion and write $\ln S =$

$\ln(1-(1-S)) \approx -(1-S)$. Equation (16) can be written as

$$v(1+c\tau)\frac{\mathrm{d}S}{\mathrm{d}x'} = \left(c - \frac{1}{s}\right)S(1-S). \qquad (17)$$

Taking $v(1+c\tau) = v_{\min} = 2\sqrt{D(c-(1/s))}$ (from the marginal stability principle), the above equation becomes

$$\frac{\mathrm{d}S}{\mathrm{d}x'} = \frac{v(1+c\tau)}{4D}S(1-S).$$

The solution is

$$S = \frac{\mathrm{e}^{\frac{v(1+c\tau)}{4D}x' + k_1}}{\mathrm{e}^{\frac{v(1+c\tau)}{4D}x' + k_1} + 1}$$

where k_1 is a constant which has to be determined. By using a trigonometric identity, we obtain

$$S = \tfrac{1}{2}\left[1 + \tanh\left(\left(\frac{v}{8D}\right)((1+c\tau)x' - x'_0)\right)\right] \qquad (18)$$

where k_1=$-vr'_0/4D$ and

$$v = \frac{2\sqrt{D(c-(1/s))}}{(1+c\tau)}. \qquad (19)$$

From our evaluations, the corresponding equations for R, E and I are related to the equation of motion of a harmonic oscillator under an external forcing: $(\mathrm{d}^2y/\mathrm{d}x'^2) + wy = F(x')$. Here y is I, R, or E. $w = c/D$ and $F(x') = (v/D)\mathrm{d}\ln S/\mathrm{d}x'$ for $y = I$. $w = -c/D, F(x') = \ln S/sD$ for $y = R$. $w = -1/v^2\tau^2, F(x') = -(1/v\tau)(\mathrm{d}S/\mathrm{d}x') - \mathrm{d}^2S/\mathrm{d}x'^2$ for $y = E$. The solutions are

$$S(x') = \tfrac{1}{2}\left[1 + \tanh\left(\left(\frac{v}{8D}\right)((1+c\tau)x' - x'_0)\right)\right]$$

$$R(x') = -\frac{1}{sc}\ln S$$

$$I(x') = \frac{v}{c}\frac{\mathrm{d}\ln S}{\mathrm{d}x'}$$

$$E(x') = 1 - S(x') - I(x') - R(x')$$

where $x'_0 = -4k_1D/v$, v is given by (19), and k_1 is any constant.

Approximate solutions in the wake of the infection wave

Now we consider the wake (rear tail) of the infection wave. The density of the recovered population can be found as follows. Consider the equation

$$\ln S + scR + sD\frac{\mathrm{d}^2R}{\mathrm{d}x'^2} = 0.$$

Far in the tail of the wave, the densities of the recovered and of the susceptibles reach their limiting values: $I = 0$, $E = 0$, $R = R^*$ = constant, and $R^* + S^* = 1$. Hence the invariant (14) takes the form $\ln S^* = sc(S^* - 1)$ or $S^* = \mathrm{e}^{sc(S^*-1)}$. This transcendental equation has the solution

$$S^* = \frac{-W_k(-S_0\sigma)}{sc} \qquad (20)$$

where $W_k(z)$ is the kth branch of the Lambert W function, the solution of $z = W_k\,\mathrm{e}^{W_k}$, $S_0 = 1$, and $\sigma = sc\,\mathrm{e}^{-sc}$. From (20), we can see that if $W_k \leqslant -1$, then S^* will have positive solutions. But if $W_k \geqslant -1$ then some values of W_k will give negative values of S^*. So W_{-1} is the only possible solution. Hence we choose W_{-1}. Using $S(x') = S^* + f(x)$ (with $f(x) \leqslant S^*$) and (17), we obtain

$$DS^*\frac{\mathrm{d}^2f}{\mathrm{d}x'^2} + (v + cv\tau S^*)\frac{\mathrm{d}f}{\mathrm{d}x'} + \left(cS^* - \frac{1}{s}\right)f = 0. \qquad (21)$$

As usual, the exponential substitution $f(x') = \mathrm{e}^{\beta x'}$, leads to $(\partial f/\partial x') = (\partial\,\mathrm{e}^{\beta x'}/\partial x') = \beta\,\mathrm{e}^{\beta x'}$ and $(\partial^2 f/\partial x'^2) = \beta^2\,\mathrm{e}^{\beta x'}$. Equation (21) can be written as

$$DS^*\beta^2 + (v + cv\tau S^*)\beta + \left(cS^* - \frac{1}{s}\right) = 0$$

which has the roots

$$\beta = -\frac{v + cv\tau S^*}{2DS^*} \pm \sqrt{\left(\frac{v + cv\tau S^*}{2DS^*}\right)^2 - \frac{CS^* - \frac{1}{s}}{DS^*}}. \qquad (22)$$

Only the positive solution has a physical meaning because S is an increasing function of x'. The full function is $S = S^* + f = S^* + c_1\,\mathrm{e}^{\beta x'}$, where c_1 is an appropriate constant. Hence

$$S = \frac{-W_{-1}(-S_0\sigma)}{sc} + c_1\,\mathrm{e}^{\beta r'}$$

where β is positive in (22). We use the approximation $W(x) \approx x - x^2 + \frac{3}{2}x^3 - \frac{8}{3}x^4 + \frac{125}{4}x^5$ and after some calculations we obtain the full solutions in the wake of infection wave:

$$S(x') = c_1\,\mathrm{e}^{\beta x'} + \frac{1}{sc}(-S_0\sigma + S_0^2\sigma^2 - \tfrac{3}{2}S_0^3\sigma^3 + \tfrac{8}{3}S_0^4\sigma^4 - \tfrac{125}{4}S_0^5\sigma^5),$$

$$R(x') = -\frac{1}{sc}\ln\left(c_1\,\mathrm{e}^{\beta x'} + \frac{1}{sc}(-S_0\sigma + S_0^2\sigma^2 - \tfrac{3}{2}S_0^3\sigma^3 + \tfrac{8}{3}S_0^4\sigma^4 - \tfrac{125}{4}S_0^5\sigma^5)\right),$$

$$I(x') = \frac{c_1 sv\beta\, \mathrm{e}^{\beta x'}}{scc_1\, \mathrm{e}^{\beta x'} - S_0\sigma + S_0^2\sigma^2 - \frac{3}{2}S_0^3\sigma^3 + \frac{8}{3}S_0^4\sigma^4 - \frac{125}{24}S_0^5\sigma^5}$$

where c_1 is a constant. The approach considered above is no longer applicable since the fast growing $f(r)$ gets large compared to S^*. However, here S itself is quite small, so one can neglect both the quadratic term and the second derivative in (21) and obtain

$$\frac{\mathrm{d}\ln S}{\mathrm{d}x'} = \frac{c}{v} + \frac{\ln S}{sc} - c\tau\frac{\mathrm{d}S}{\mathrm{d}x'}.$$

Taking the exponential solution of the above equation, the solutions for the tail of the infection wave are

$$S(x') = \exp\left(k_2\, \mathrm{e}^{\frac{x'}{sv(1+c\tau)}} - sc\right)$$

$$R(x') = -\frac{1}{sc}\ln S = -\frac{k_2}{sc}\, \mathrm{e}^{\frac{x'}{sv(1+c\tau)} - sc}$$

$$I(x') = \frac{v}{c}\frac{\mathrm{d}\ln S}{\mathrm{d}x'}$$

$$E(x') = 1 - S(x') - I(x') - R(x')$$

where k_2 is a constant.

The solutions are calculated and plotted using MATLAB. Parameters used in the model (3)–(6) are: c (the rate constant of the transmission of the disease from infectious to susceptible humans) = 0.6, 0.8, and 0.1; D (diffusion coefficient) = 1 km^2/day; τ (intrinsic incubation time) = 6.8, 8, 10, 15, 20 days; s (recovery time) = 3, 5, 15, 20, 25 days.

We examine the change in shape of the disease wave under variation of the contact and recovery rates. Figs. 1 and 2 represent the shape of the wave for the different contact rates. The shape of the wave is shown in Figs. 3 and 4 for the different recovery rates. In all of these cases, both front and back solutions show exponential types of behaviour. The exponential decrement of the front solutions exhibits a rather small change.

From Figs. 1–4, we can see that the epidemic peak, the time of the epidemic peak ($t_{\max}$) and the length of outburst are different. The individual population for the higher contact rate and lower recovery rates (the longer duration for recovering) produce the higher epidemic peak, $t_{\max}$ and length of the epidemic outburst. As we see in Figs. 1–4, the peaks of the exposed individuals for both front and back solutions are higher than the peaks of the infectious ones because some exposed individuals recover before they become infectious. Furthermore, the distances from criticality in these three waves are different because the product of c and s is different.

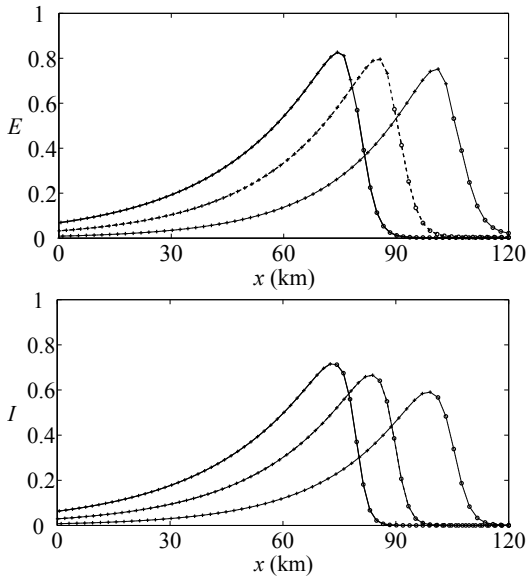

Fig. 1 The spatial solutions for the different contact rates of exposed and infectious populations (left curve: $c = 1$, $v = 0.15$; middle curve: $c = 0.8$, $v = 0.17$; right curve: $c = 0.6$, $v = 0.18$) for $t = 700$ days. Fixed parameters: $\tau = 10$ days, $s = 15$ days. For this and the next 5 figures: + shows the wake solution; o shows the front solution; solid line shows the approximate solution.

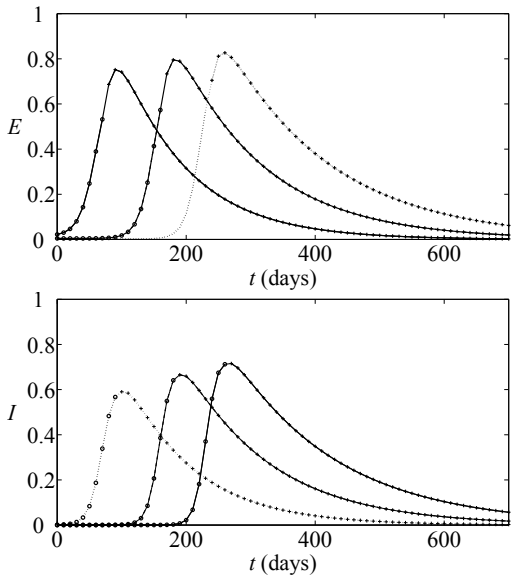

Fig. 2 The time series solutions for the different contact rates of exposed and infectious populations (left curve: $c = 0.6$, $v = 0.18$; middle curve: $c = 0.8$, $v = 0.17$; right curve: $c = 1$, $v = 0.15$) for $x = 120$. Fixed parameters: $\tau = 10$ days, $s = 15$ days. $t_{\max} = 101$, 188, and 264 days for $c = 0.6$, 0.8, and 1, respectively.

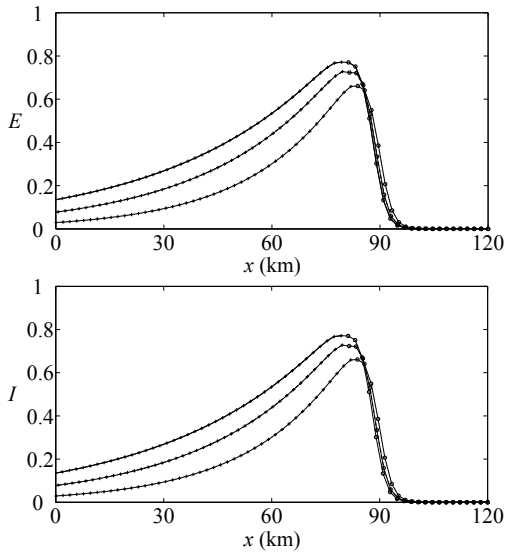

Fig. 3 The spatial solutions for the different recovery rates of exposed and infectious populations (top curve: $s = 25$, $v = 0.1648$; middle curve: $s = 20$, $v = 0.1667$; bottom curve: $s = 15$, $v = 0.1678$) for $t = 700$ days. Fixed parameters: $\tau = 10$ days, $c = 0.8$.

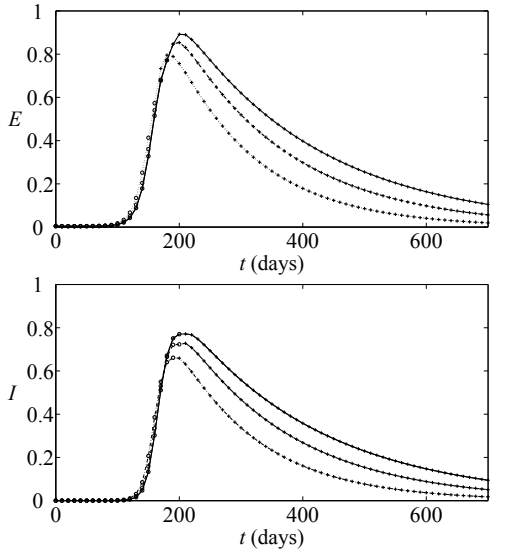

Fig. 4 The time series solutions for the different recovery rates of exposed and infectious populations (top curve: $s = 25$, $v = 0.1648$; middle curve: $s = 20$, $v = 0.1667$; bottom curve: $s = 15$, $v = 0.1678$) for $x = 120$. Fixed parameters: $\tau = 10$ days, $c = 0.8$. $t_{\max} = 190$, 200, and 210 days for $s = 15$, 20, and 25, respectively.

Figs. 5 and 6 show the shapes of the waves for the different values of parameters with the same velocity. We can see that with fixed velocities, the

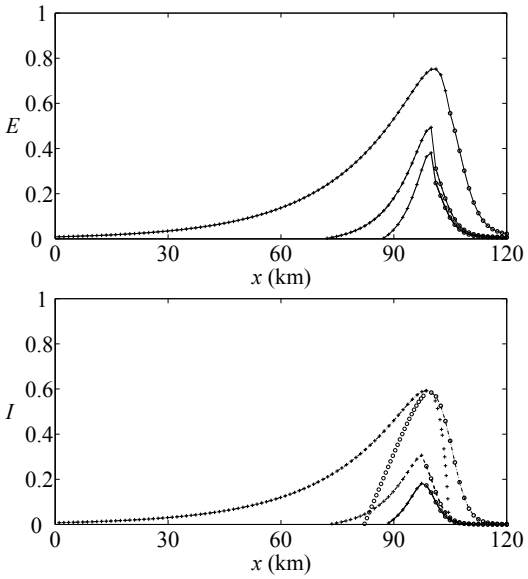

Fig. 5 The spatial solutions for the different values of parameters with the same velocity ($v = 0.2$) of exposed and infectious populations (top curve: $c = 0.6$, $s = 15$, $\tau = 10$; middle curve: $c = 0.8$, $s = 5$, $\tau = 8$; bottom curve: $c = 1$, $s = 3$, $\tau = 6.8$) for $t = 700$ days. The complete trailing and leading edges set of points have been plotted for the infectious human proportion solution for the parameter values [$c = 0.6$; $s = 15$; $\tau = 10$].

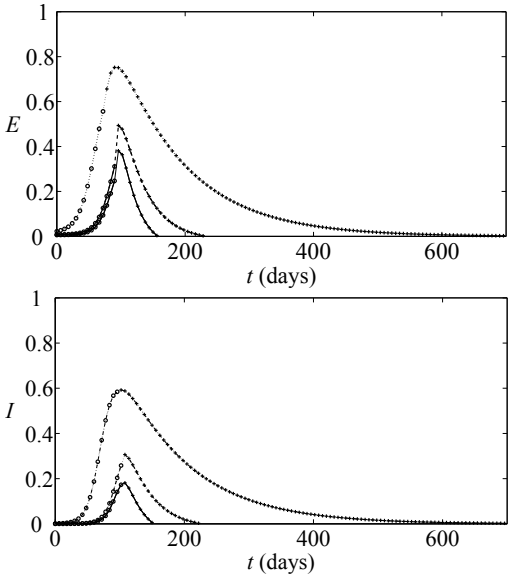

Fig. 6 The time series solutions for the different values of parameters with the same velocity ($v = 0.2$) of exposed and infectious populations (top curve: $c = 0.6$, $s = 15$, $\tau = 10$; middle curve: $c = 0.8$, $s = 5$, $\tau = 8$; bottom curve: $c = 1$, $s = 3$, $\tau = 6.8$) for $x = 120$.

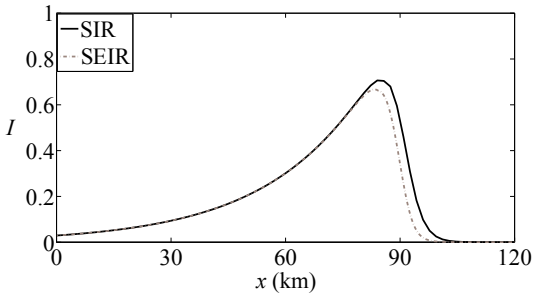

Fig. 7 The spatial solution of an infectious human population from SIR and SEIR models compared ($c = 0.8$, $s = 15$ days).

shapes of the waves give the same time for the epidemic peaks but different slopes of the curves. On all figures, the solid line is obtained by connecting points from the numerical solutions of the analytical (approximate) solutions. The left side part is made from points coming from the 'wake' solution, while the right part is made from points coming from the 'leading front' solution. These two curves intersect, and the choice of how long we keep the wake values before switching to the leading front values is made automatically to ensure the smoothest curve, which is the most physical. An exact solution, if it could be found, would have a smooth behaviour, but it is difficult to obtain as our calculations are possible only under the approximation that the second derivative can be neglected. This approximation fails near the maximum. Hence we make a smooth junction of the front and wake solutions. To illustrate this, we show more values of the trailing and leading solutions on one of the curves of Fig. 5, which is the case for which the junction is the least smooth.

The comparison of infection waves from SIR and SEIR models ((3)–(6)) is shown in Fig. 7. We can see that the peak of infection wave in the SEIR model is less than the peak of infection wave in the SIR model. The length of the outburst in the SEIR model is also less than the length of the outburst in the SIR model.

CONCLUSIONS

We considered the spread of exposed and infectious populations in a contact mode of the propagation of the disease in which the populations have only local motions. The corresponding analytical solutions are obtained and the solution shows a propagating wave of asymmetric shape. We compared these analytical solutions for the different ranges of parameters. We show that the dynamics of the SEIR model is slower than that of an SIR model, and that the total proportion of infectious cases is substantially smaller. Although it is not really surprising *per-se*, as the transition through the additional exposed class takes time, it is real progress to be able to quantify the differences, especially as it may allow curative measures to be decided in order to limit an epidemic outburst.

Acknowledgements: This work received financial support from the Franco-Thai collaborative research programme (2009/2010), the MATECLID project (APR GICC 2002), and the EPIDENGUE project (ANR 00119 05). D.G.L. has a PhD grant from the French Ministère de la Recherche. We also thank a referee for useful suggestions, and we owe a lot to Michael A. Allen who pointed out a major blunder.

REFERENCES

1. Diekmann O, Heersterbeek H (2000) *Mathematical Epidemiology of Infectious Disease*, Wiley, New York.
2. Murray J (2003) *Mathematical Biology II*, Springer.
3. Kendall DG (1965) Mathematical models of the spread of infection. In: *Mathematics and Computer Science in Biology and Medicine*, HMSO, London.
4. Liu WM, Hethcote HW, Levin SA (1987) Dynamical behavior of epidemiological models with nonlinear incidence rate. *J Math Biol* **25**, 359–80.
5. Greenhalgh D (1992) Some results for an SEIR epidemic model with density dependence in the death rate. *IMA J Math Appl Med Biol* **9**, 67–106.
6. Li MY, Muldowney JS (1995) Global stability for the SEIR model in epidemiology. *Math Biosci* **125**, 155–64.
7. Zhang J, Ma Z (2003) Global dynamic of SEIR epidemic model with saturating contact rate. *Math Biosci* **185**, 15–32.
8. Korobeinikov A (2004) Lyapunov functions and global properties for SEIR and SEIS epidemic models. *J Math Biol* **21**, 75–83.
9. Li G, Jin Z (2005) Global stability of an SEI epidemic model with general contact rate. *Chaos Soliton Fract* **23**, 997–1004.
10. Brunet E, Derrida B (1997) Shift in the velocity of a front due to a cutoff. *Phys Rev E* **56**, 2597–604.
11. Mai J, Sokolov IG, Blumen A (1998) Discreteness effects on the front propagation in the A+B $\rightarrow$ 2A reaction in 3 dimensions. *Europhys Lett* **44**, 7–12.
12. Gourley SA, Liu R, Wu J (2007) Some vector borne diseases with structured host populations: extinction and spatial spread. *SIAM J Appl Math* **67**, 408–33.
13. Postnikov EB, Sokolov IM (2007) Continuum description of a contact infection spread in a SIR model. *Math Biosci* **208**, 205–15.
14. Naether U, Postnikov EB, Sokolov IM (2008) Infection fronts in contact disease spread. *Eur Phys J B* **65**, 353–9.